Hindawi
Complexity
Volume 2023, Article ID 6751849, 10 pages
https://doi.org/10.1155/2023/6751849

Research Article

Protocol-Based Reliable Control for Power Systems with Communication Constraints

Yong Chen, Meng Li, Song Li, Yunhui Wang, Min Xie, and Yongkun Yang

Infrastructure Department of Yunnan Power Grid Company Limited, China Southern Power Grid, LTD., Kunming, Yunnan 650000, China

Correspondence should be addressed to Yong Chen; 1033687453@qq.com

Received 8 November 2022; Revised 20 December 2022; Accepted 5 April 2023; Published 22 April 2023

Academic Editor: Fuli Zhou

Copyright © 2023 Yong Chen et al. This is an open access article distributed under the Creative Commons Attribution License, which permits unrestricted use, distribution, and reproduction in any medium, provided the original work is properly cited.

This study focuses on the protocol-based control for single-area power systems subject to actuator failures and deception attacks. Specifically, actuator failures, network attacks, unreliability, and bandwidth restrictions that emerge in power systems are taken into consideration at the same time. To cut down on the number of broadcast packets, a novel memory-adaptive event-triggered protocol is developed, where the trigger threshold parameter is adaptively changed in accordance with numerous historical sampled signals. Then, in virtue of the proposed algorithm, sufficient stabilization conditions are acquired to ensure the asymptotically stable of power systems with H_∞ performance. Finally, the efficiency of the proposed control strategy is demonstrated by using a simulation example.

1. Introduction

Due to its potent capacity to change the system frequency to a predetermined value in the presence of load fluctuations, load frequency control (LFC) has been utilized successfully in power systems for several decades [1–3]. Modern LFC in power systems transmits control signals and measured values across open communication networks (OCNs) as opposed to classic LFC, which transfers data over specialized communication channels. As the size of the power system grows, data transmission over a dedicated communication channel in traditional LFC will increase maintenance costs and reduce flexibility; hence, modern LFC with OCNs is becoming more popular [4]. However, as OCNs are prone to data loss, network attacks, and communication delay, data transfer through them might present considerable difficulties. Consequently, there has been a lot of interest in the study and development of LFC schemes for power systems with OCNs (see, for more details, [5–7]).

Actuators are crucial components of networked control systems, and it is a common phenomenon that a variety of malfunctions occur, which may affect the system performance [8]. In this regard, for the purpose of guaranteeing the desired performance, a seemingly natural ideal is to introduce reliable control schemes. As discussed in [9], benefiting from the reliable control schemes, actuator failures can be compensated and avoided. As a consequence, a lot of focus has been placed on the research of actuator failures in an effort to address these shortcomings and boost dependability, and several findings have been published [10, 11]. The finite-time tracking control problem for nonlinear systems with faults has been studied in [10]. Besides, the fault-tolerant control problem for multiagent systems subject to DoS attacks has been exploited in [11]. However, reliable control schemes have not gained sufficient interest in power systems probably due to dynamic complexities including unknown perturbations. To date, despite considerable accomplishments, power systems subject to reliable control schemes are still in their infancies, which remain the first motivation for this study.

It is essential to mention that communication networks are large-scale and decentralized and that the links between each part of a networked power system might make them vulnerable to cyberattacks [12]. According to [13], cyberattacks can have significant negative effects on system performance, such as information leaks, system failures, and financial losses. Additionally, control methods might be used as a compensating strategy since cyber security approaches are insufficient to secure power systems [14]. Among some control methods, denial-of-service (DoS) attacks and deception attacks have generated a lot of research attention [11, 15–18]. Some common concepts or solutions have been carried out for DoS attacks. From the point of adversary, DoS attacks have been described by stochastic models, i.e., the Bernoulli method [19] and Markov method [20]. Additionally, from the standpoint of the attacker, deception attack can alter data to compromise its integrity, and the time-varying attack behavior cannot be detected [21]. As a result, the study of deception attacks becomes more challenging ([14, 18, 22]). Following this trend, a seemingly natural research topic is established for security control of networked power systems, which gives rise to deception attacks.

In light of the limited communication capacity, a range of networked phenomena emerged. In response to communication networks with constrained network resources, two transmission strategies are most adopted: the time-triggered protocol [23–25] and the event-triggered protocol [26, 27]. Note that conventional TTPs may result in wasted network resources; the event-triggered protocol has been developed in recent years to address these issues. Because trigger conditions are carried out after the event as opposed to before it, ETPs typically use fewer system resources than TTP. In general, the existing ETPs can be classified into static event-triggered protocols (SETPs) [15, 28], dynamic event-triggered protocols (DETPs) [29–31], and adaptive event-triggered protocols (AETPs) [32, 33]. For AETPs, threshold functions, based on the evolution of system states, are updated adaptively. Although there are several AETPs with dynamically changed threshold functions, there is still significant potential for development. For instance, in [32, 33], the threshold function is built using a quantitative relationship with the error between the latest transmitted data and the currently sampled data. Inspired by the work of the authors of [34], the aforementioned approach can be improved by containing the historically transmitted packets in the threshold function. Furthermore, memory-based AETPs have not gained proper research interest in power systems, which prompts us to the current study.

In light of the description above, this study examines the based-protocol LFC problem for single-area power systems (SAPSs) that are vulnerable to deception attacks and actuator failures. The following is a summary of our paper's main points: (1) A memory-adaptive event-triggered protocol (MAETP) is presented for operating SAPSs across communication networks with constrained bandwidth. Meanwhile, the MAETP accomplishes the goal of memory by dynamically altering the adaptive parameters using historical trigger data while preserving the intended control performance. (2) The proposed SAPS results account for a common framework together with the effects of deception attacks, actuator faults, and memory-based event-triggered protocols. (3) For the established power system model, according to the Lyapunov stability method, the asymptotic stability (AS) with preset performance is ensured.

2. Problem Formulations

2.1. System Model. Throughout the study, the dynamic model of a single-area power system is described as follows [35]:

$$\left\{ \dot{\tilde{x}}(t) = \tilde{A}\tilde{x}(t) + \tilde{B}u^F(t) + \tilde{H}v(t), \tilde{y}(t) = \tilde{C}\tilde{x}(t), \right. \tag{1}$$

where

$$\begin{aligned}
\tilde{x}(t) &= \begin{bmatrix} \Delta f & \Delta P_v & \Delta P_m \end{bmatrix}^\top, \\
\tilde{y}(t) &= ACE, \\
v(t) &= \Delta P_d, \\
\tilde{A} &= \begin{bmatrix} -\frac{D}{M} & 0 & \frac{1}{M} \\ -\frac{1}{RT_g} & -\frac{1}{T_g} & 0 \\ 0 & \frac{1}{T_t} & -\frac{1}{T_t} \end{bmatrix}, \\
\tilde{B} &= \begin{bmatrix} 0 \\ \frac{1}{T_g} \\ 0 \end{bmatrix}, \\
\tilde{H} &= \begin{bmatrix} -\frac{1}{M} \\ 0 \\ 0 \end{bmatrix}, \\
\tilde{C} &= \begin{bmatrix} \beta & 0 & 0 \end{bmatrix}.
\end{aligned} \tag{2}$$

Table 1 provides a list of parameters' physical meanings.

Note that, for a single-area power system without power exchange, the ACE signal is written as $ACE = \beta\Delta f$, where β is frequency bias. In actual fact, actuator failures cannot be ignored, so the failure model between the controller and the actuator is represented as follows:

$$u^F(t) = \rho u(t), \tag{3}$$

where $\rho = \text{diag}\{\rho_1, \rho_2, \cdots, \rho_{n_u}\}$ and $0 \le \underline{\varrho}_m \le \varrho_m \le \overline{\varrho}_m \le 1$ $(m = 1, 2, \cdots, n_u)$, in which ρ_m is unknown, and we assume

Table 1: The physical meaning of parameters.

Parameters	Physical meaning
Δf	The deviation of frequency
ΔP_m	The deviation of governor mechanical output increment
ΔP_v	The valve position deviation
ΔP_d	Load disturbance
ACE	Area control error
D	Governor damping coefficient
M	Rotational inertia
T_t	Turbine time constant
T_g	Governor time constant
R	Droop property

that $\underline{\varrho}_m$ and $\overline{\varrho}_m$ are known. We define $\underline{\varrho} = \min\left\{\underline{\varrho}_m, m = 1, 2, \cdots, n_u\right\}$ and $\overline{\varrho} = \max\{\overline{\varrho}_m, m = 1, 2, \cdots, n_u\}$.

As a consequence, a PI controller is inferred as

$$u(t) = -K_P ACE - K_I \int ACE. \tag{4}$$

Furthermore, we define state vectors as $x(t) = \left[\Delta f \;\; \Delta P_v \;\; \Delta P_m \;\; \int ACE\right]^{\mathrm{T}}$ and measured output as $y(t) = \left[ACE \int ACE\right]$; the dynamic model of the single-area power system is redescribed as

$$\begin{cases} \dot{x}(t) = Ax(t) + B\rho u(t) + Hv(t), \\ y(t) = Cx(t), \end{cases} \tag{5}$$

where

$$A = \begin{bmatrix} -\frac{D}{M} & 0 & \frac{1}{M} & 0 \\ -\frac{1}{RT_g} & -\frac{1}{T_g} & 0 & 0 \\ 0 & \frac{1}{T_t} & -\frac{1}{T_t} & 0 \\ \beta & 0 & 0 & 0 \end{bmatrix},$$
$$B = \begin{bmatrix} 0 \\ \frac{1}{T_g} \\ 0 \\ 0 \end{bmatrix},$$
$$H = \begin{bmatrix} -\frac{1}{M} \\ 0 \\ 0 \\ 0 \end{bmatrix},$$
$$C = \begin{bmatrix} \beta & 0 & 0 & 0 \\ 0 & 0 & 0 & 1 \end{bmatrix}. \tag{6}$$

2.2. Memory-Adaptive Event-Triggered Protocol. By using some historical data, a sampling-based MAETP is proposed in [34]:

$$t_{k+1}h = t_k h + \inf_{l \in \mathbb{N}^+} \left\{ lh \mid e^\top(t)\Omega e(t) - \sigma(t) y^\top(t_k h)\Omega y(t_k h) \geq 0 \right\}, \tag{7}$$

and $e(t) = y(t_k h + lh) - y(t_k h)$. h, kh, and $t_k h$ describe the sampling interval, instant, and latest broadcast instant, respectively. The matrix $\Omega > 0$. Meanwhile, $\{t_k h, k \in \mathbb{N}^+\} \subseteq \{kh, k \in \mathbb{N}^+\}$. In the sequel, the adaptive parameter $\sigma(t)$ yields

$$\sigma(t) = \sigma + \left(\overline{\sigma} - \sigma\right) e^{-\epsilon \left\| y(t_k h + lh) - \frac{1}{\mathcal{S}} \sum_{s=1}^{\mathcal{S}} y(t_{k-s} h) \right\|^2}, \tag{8}$$

where σ and $\overline{\sigma}$ indicate two bounds of the adaptive threshold parameters, $\epsilon > 0$, and $\mathcal{S}$ is the number of recent released packets.

Remark 1. Note that the adaptive threshold function of MAETP (7) taken into consideration in this study, which substitutes the latest trigger sample with the arithmetic mean of $\mathcal{S}$ historically trigger data, can lessen the sensitivity of $\sigma(t)$ to the most latest transmitted data $y(t_k h)$. As in [18], the proposed controller gain number is $\mathcal{S}$, which increases the computing cost if the amount of historical data is too large. To avoid this situation, the MAETM proposed in this research adds the memory feature to the adaptive rule.

Remark 2. In addition to providing flexibility in modifying the trigger threshold, the MAETP (7) also improves control performance. Nevertheless, the MAETP (5) provided in this research is more inclusive and covers the majority of the current protocols. When $\mathcal{S} = 1$, MAETPs (7) reduce to AETPs [32]. When $\mathcal{S} = 1$ and $\sigma(t)$ is a constant, the MAETP (7) degenerates to SETPs [15]. Following this fact, the designed DMETP is more appropriate than the current SETP/AETP to describe the actual scenario.

Considering the delay in transmitting data, we define the transmission interval as $\bigcup_{l=0}^{n} \mathcal{I}_l = [t_k h + d_k, t_{k+1} h + d_{k+1}]$, and one gets $\mathcal{I}_l = [t_k h + lh + d_{k+l}, t_{k+1} h + lh + h + d_{k+l+1}]$ and $(l = 0, 1, \cdots, n, n = t_{k+1} - t_k - 1)$. We set $d(t) = t - t_k h - lh$, which yields

$$0 \leq d(t) \leq h + \overline{d} \triangleq d_M, \tag{9}$$

where $\overline{d}$ is the upper bound of $\{d_k\}$.

Summarizing the aforementioned analysis, we let $K = [-K_P \ \ -K_I]$. Under the MAETP, the PI controller is rewritten as

$$u(t) = K y(t_k h). \tag{10}$$

As a follow-up, the measurement output is assumed to be attacked by random deception attacks. In this regard, the load frequency controller is remodelled as

$$u(t) = (1 - \alpha(t)) K y(t_k h) + \alpha(t) K f(t_k h), \tag{11}$$

where the nonlinear function $f(t_k h)$ indicates the deception signal. $\alpha(t) \in \{0, 1\}$ is a Bernoulli random variable, from which one has

$$\begin{aligned} \Pr\{\alpha(t) = 1\} &= \mathbb{E}\{\alpha(t)\} \\ &= \overline{\alpha}, \\ \Pr\{\alpha(t) = 0\} &= 1 - \overline{\alpha}. \end{aligned} \tag{12}$$

Assumption 1 (see [15]). It is assumed that the nonlinear function can be characterized by the following condition:

$$\| f(y(t)) \| \leq \| F(y(t)) \|, \tag{13}$$

where F is a known matrix.

Substituting (11) into (5), the closed-loop power system can be established as

$$\begin{cases} \dot{x}(t) = A x(t) + \rho(1 - \alpha(t)) B K (C x(t - d(t)) - e(t)) + \rho \alpha(t) B K f(y(t_k h)) + H v(t), \\ y(t) = C x(t). \end{cases} \tag{14}$$

In order to solve static output-feedback control questions, we let $\mathcal{B} = [B \ \ \overline{B}]$, in which $\overline{B}$ has $4 - p$ [36]. Then, we introduce a new variable $\chi(t) = (\widehat{B})^{-1} x(t)$; system (15) is reformulated as

$$\begin{cases} \dot{\chi}(t) = \mathcal{A}\chi(t) + \rho(1 - \alpha(t)) \mathcal{K}(\mathcal{C}\chi(t - d(t)) - e(t)) + \rho\alpha(t)\mathcal{K} f(y(t_k h)) + \mathcal{H} v(t), \\ y(t) = \mathcal{C}\chi(t), \end{cases} \tag{15}$$

where $\mathcal{A} = (\mathcal{B})^{-1} A \mathcal{B}$, $\mathcal{K} = [K^\top 0]^\top$, $\mathcal{C} = C\mathcal{B}$, and $\mathcal{H} = \mathcal{B}^{-1} H$.

The goal of this paper is to construct the controller (11) in such a way that it satisfies asymptotically stable subjects to preset performance for the closed-loop power system (16) under MAETPs (7). In particular, the following requirements are met:

1) The closed-loop power system (16) with $v(t) = 0$ is AS.

2) Under zero initial conditions, it holds that $\mathscr{E}\left\{\int_0^\infty \|y(t)\|^2 dt\right\} < \gamma^2 \mathscr{E}\left\{\int_0^\infty \|v(t)\|^2 dt\right\}$ for all $v(t) \neq 0$ and prescribed $\gamma > 0$.

Lemma 1 (see [37]). *For any matrices* $\mathscr{R} \in \mathbb{R}^{n\times n}$ *and* $\mathscr{U} \in \mathbb{R}^{n\times n}$, *we satisfy* $\begin{bmatrix} \mathscr{R} & * \\ \mathscr{U} & \mathscr{R} \end{bmatrix} > 0$, $d(t) \in [0, d_M]$, *with* $d_M \geq 0$, *and the vector function* $\dot{x}$: $[0, d_M] \longrightarrow \mathbb{R}^n$; *the following condition holds*

$$-d_M \int_{t-d_M}^{t} \dot{x}^\top(s)\mathscr{R}\dot{x}(s)ds \leq -\zeta^\top(t)\Lambda\zeta(t), \tag{16}$$

where $\zeta(t) = col[x(t), x(t-d(t)), x(t-d_M)]$ *and* $\Lambda = \begin{bmatrix} \mathscr{R} & * & * \\ \mathscr{U}-\mathscr{R} & 2\mathscr{R}-\mathbf{He}\{\mathscr{U}\} & * \\ -\mathscr{U} & \mathscr{U}-\mathscr{R} & \mathscr{R} \end{bmatrix}$.

3. Main Results

Theorem 1. *For given scalars* $d_M \geq 0$, $\overline{\sigma} \in (0,1)$, $\iota > 0$, $\epsilon > 0$, $\overline{\rho}$, *and* $\rho \in [0,1]$, *the closed-loop power system (16) is AS in the sense of the* H_∞ *performance index* γ *if there exist matrices* $P > 0$, $Q > 0$, $R > 0$, *and* $\Omega > 0$ *and matrices* U *and* $\mathscr{M}$ *such that*

$$\begin{bmatrix} R & U^\top \\ U & R \end{bmatrix} > 0, \tag{17}$$

$$\begin{bmatrix} \Xi^1 & \Xi^2 & \Xi^3 & \Xi^4 \\ * & -\gamma^2 I & 0 & 0 \\ * & * & -\overline{\alpha}I & 0 \\ * & * & * & -I \end{bmatrix} < 0, \tag{18}$$

where

$$\begin{aligned}
\Xi^1 &= \begin{bmatrix} \Xi^{1,1} & \Xi^{1,2} \\ * & \Xi^{2,2} \end{bmatrix}, \\
\Xi^2 &= \begin{bmatrix} \mathscr{H}^\top\mathscr{M}^\top & 0 & 0 & \iota\mathscr{H}^\top\mathscr{M}^\top & 0 & 0 \end{bmatrix}^\top, \\
\Xi^3 &= \begin{bmatrix} 0 & \overline{\alpha}\mathscr{F}\mathscr{C} & 0 & 0 & \overline{\alpha}\mathscr{F}\mathscr{C} & 0 \end{bmatrix}^\top, \\
\Xi^4 &= \begin{bmatrix} \mathscr{C} & 0 & 0 & 0 & 0 & 0 \end{bmatrix}^\top, \\
\Xi^{1,1} &= \begin{bmatrix} \Upsilon^{11} & \Upsilon^{12} & U^\top \\ * & -2R + U^\top + U + \overline{\sigma}\mathscr{C}^\top\Omega\mathscr{C} & R - U^\top \\ * & * & -R - Q \end{bmatrix}, \\
\Xi^{1,2} &= \begin{bmatrix} \Upsilon^{14} - \rho(1-\overline{\alpha})\mathscr{M}\mathscr{K} & \overline{\rho}\overline{\alpha}\mathscr{M}\mathscr{K} & \\ \iota\overline{\rho}(1-\overline{\alpha})(\mathscr{M}\mathscr{K}\mathscr{C})^\top & -\overline{\sigma}\mathscr{C}^\top\Omega & 0 \\ 0 & 0 & 0 \end{bmatrix}, \\
\Xi^{2,2} &= \begin{bmatrix} d_M^2 R - \mathbf{He}\{\iota\mathscr{M}\} - \iota\rho(1-\overline{\alpha})\mathscr{M}\mathscr{K} & \iota\overline{\rho}\overline{\alpha}\mathscr{M}\mathscr{K} & \\ * & (\overline{\sigma}-1)\Omega & 0 \\ * & * & -\overline{\alpha}I \end{bmatrix}, \\
\Upsilon^{11} &= \mathbf{He}\{\mathscr{M}\mathscr{A}\} + Q - R, \\
\Upsilon^{12} &= \overline{\rho}(1-\overline{\alpha})\mathscr{M}\mathscr{K}C - U^\top + R, \\
\Upsilon^{14} &= P - \mathscr{M}^\top + \iota\mathscr{A}^\top\mathscr{M}^\top.
\end{aligned} \tag{19}$$

Proof. Considering the following Lyapunov function,

$$V(t) = \sum_{l=1}^{3} V_l(t), \tag{20}$$

where

$$\begin{aligned}
V_1(t) &= \chi^\top(t)P\chi(t), \\
V_2(t) &= \int_{t-d_M}^{t} \chi^\top(s)Q\chi(s)ds, \\
&= d_M \int_{-d_M}^{0}\int_{t+s}^{t} \dot{\chi}^\top(v)R\dot{\chi}(v)dv\,ds.
\end{aligned} \tag{21}$$

Taking the derivative of $V(t)$, one has

$$\begin{aligned}
\mathscr{L}V_1(t) &= 2\dot{\chi}^\top(t)P\chi(t), \\
\mathscr{L}V_2(t) &= \chi^\top(t)Q\chi(t) - \chi^\top(t-d_M)Q\chi(t-d_M), \\
\mathscr{L}V_3(t) &= d_M^2\dot{\chi}^\top(t)R\dot{\chi}(t) - d_M\int_{t-d_M}^{t} \dot{\chi}^\top(s)R\dot{\chi}(s)ds.
\end{aligned} \tag{22}$$

Based on Lemma 1, it follows

$$-d_M\int_{t-d_M}^{t} \dot{\chi}^\top(s)R\dot{\chi}(s)ds \leq -\zeta^\top(t)\mathscr{R}\zeta(t), \tag{23}$$

where

$$\mathscr{R} = \begin{bmatrix} R & * & * \\ U - R & 2R - \mathbf{He}\{U\} & * \\ -U & U - R & R \end{bmatrix},$$
$$\zeta(t) = \begin{bmatrix} \chi(t) \\ \chi(t - d(t)) \\ \chi(t - d_M) \end{bmatrix}. \quad (24)$$

Reviewing the established MAETP in (7), it holds that

$$\begin{aligned} 0 &< \sigma(t) y^{\top}(t_k h)\Omega y(t_k h) - e^{\top}(t)\Omega e(t), \\ &< \overline{\sigma} y^{\top}(t_k h)\Omega y(t_k h) - e^{\top}(t)\Omega e(t). \end{aligned} \quad (25)$$

Recalling (15), for any proper matrix Z, it holds that

$$0 = 2\left[\chi^{\top}(t)\mathscr{M} + \iota\dot{\chi}^{\top}(t)\mathscr{M}\right] \times \left[-\dot{x}(t) + \mathscr{A}\chi(t) + (1 - \alpha(t))\mathscr{K}(\mathscr{C}\chi(t - d(t)) - e(t)) + \alpha(t)\mathscr{K} f(y(t_k h)) + \mathscr{H} v(t)\right]. \quad (26)$$

Then, based on Assumption 1, one has

$$\overline{\alpha}\left[f^{\top}(y(t_k h)) f(y(t_k h)) - y^{\top}(t_k h)\mathscr{F}^{\top}\mathscr{F} y(t_k h)\right] \leq 0. \quad (27)$$

Taking (20)–(27) into account, we have that

$$\mathscr{L}V(t) \leq \zeta^{\top}(t)\overline{\Xi}\zeta(t) - y^{\top}(t)y(t) + \gamma^2\omega^{\top}(t)v(t), \quad (28)$$

where $\zeta^{\top}(t) = [\chi^{\top}(t)\chi^{\top}(t - d(t))\chi^{\top}\ (t - d_M)\dot{\chi}^{\top}(t)e^{\top}(t)f^{\top}(y(t_k h))\omega^{\top}(t)]$, $\overline{\Xi} = \begin{bmatrix} \Xi^1 + (1/\alpha)\Xi^3\Xi^{3,\top} + \Xi^4\Xi^{4,\top} & \Xi^2 \\ * & -\gamma^2 I \end{bmatrix}$.

Applying the Schur complement to (19), one has

$$\mathscr{L}V(t) + \|y(t)\|^2 - \gamma^2\|v(t)\|^2 \leq 0. \quad (29)$$

Integrating (29) from $t = 0$ to ∞ yields

$$V(\infty) - V(0) + \mathscr{E}\left\{\int_0^{\infty}\left(\|y(t)\|^2 - \gamma^2\|v(t)\|^2\right)\mathrm{dt}\right\} \leq 0. \quad (30)$$

Under zero initial conditions, the following inequality holds:

$$\mathscr{E}\left\{\int_0^{\infty}\left(\|y(t)\|^2 - \gamma^2\|v(t)\|^2\right)\mathrm{dt}\right\} \leq 0. \quad (31)$$

Furthermore, we get $\mathscr{E}\left\{\int_0^{\infty}\|y(t)\|^2\mathrm{dt}\right\} \leq \gamma^2\mathscr{E}\left\{\int_0^{\infty}\|v(t)\|^2\mathrm{dt}\right\}$. When $\omega(t) = 0$, we can deduce the closed loop power system (16) AS by applying condition (19). This ends the proof.

Next, Theorem 2 presents essential conditions for designing the controller gain based on the conclusion of Theorem 1. □

Theorem 2. *For given scalars $d_M \geq 0$, $\overline{\sigma} \in (0, 1)$, $\iota > 0$, $\epsilon > 0$, $\overline{\rho}$, and $\rho \in [0, 1]$, the closed-loop power system (16) is AS in the sense of the H_{∞} performance index γ if there exist matrices $P > 0$, $Q > 0$, $R > 0$, and $\Omega > 0$ and matrices U and Z with compatible dimensions such that (18) holds and*

$$\begin{bmatrix} \overline{\Xi}^1 & \Xi^2 & \Xi^3 & \Xi^4 \\ * & -\gamma^2 I & 0 & 0 \\ * & * & -\alpha I & 0 \\ * & * & * & -I \end{bmatrix} < 0, \quad (32)$$

where

$$\begin{aligned}
\overline{\Xi}^1 &= \begin{bmatrix} \overline{\Xi}^{1,1} & \overline{\Xi}^{1,2} \\ * & \overline{\Xi}^{2,2} \end{bmatrix}, \\
\Xi^{1,1} &= \begin{bmatrix} \Upsilon^{11} & \overline{\Upsilon}^{12} & U^{\top} \\ * & -2R + U^{\top} + U + \overline{\sigma}\mathscr{C}^{\top}\Omega\mathscr{C} & U^{\top} - R \\ * & * & -R - Q \end{bmatrix}, \\
\overline{\Xi}^{1,2} &= \begin{bmatrix} \Upsilon^{14} - \rho(1 - \overline{\alpha})\mathscr{Y}\mathscr{K} & \overline{\rho}\alpha\mathscr{Y}\mathscr{K} \\ \iota\overline{\rho}(1 - \overline{\alpha})(\mathscr{Y}\mathscr{K}\mathscr{C})^{\top} & -\overline{\sigma}\mathscr{C}^{\top}\Omega & 0 \\ 0 & 0 & 0 \end{bmatrix}, \\
\overline{\Xi}^{2,2} &= \begin{bmatrix} d_M^2 R - \mathbf{He}\{\iota\mathscr{M}\} - \iota\rho(1 - \overline{\alpha})\mathscr{Y}\mathscr{K} & \iota\overline{\rho}\alpha\mathscr{Y}\mathscr{K} \\ * & (\overline{\sigma} - 1)\Omega & 0 \\ * & * & -\overline{\alpha} I \end{bmatrix}, \\
\Upsilon^{12} &= \overline{\rho}(1 - \overline{\alpha})\mathscr{Y}\mathscr{K}\mathscr{C} - U^{\top} + R, \\
\mathscr{Y} &= \mathrm{diag}\{I_p, 0\}.
\end{aligned} \quad (33)$$

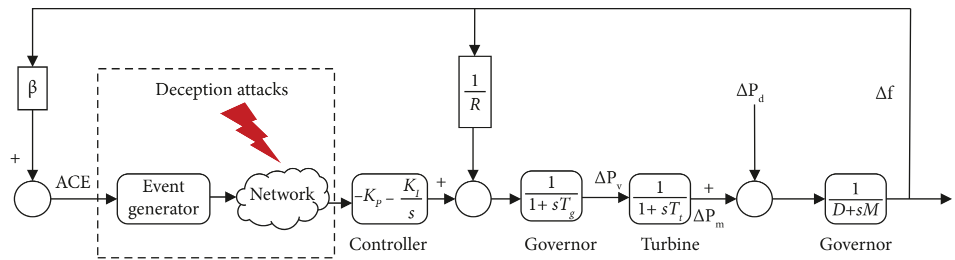

FIGURE 1: Dynamic mode of the single-area power system under deception attacks.

TABLE 2: Parameters of the power system.

M	D	T_t	T_g	β	R
10	1	0.3	0.1	21	0.05

Furthermore, the gains can be computed as

$$\mathscr{K} = \mathscr{M}^{-1}\mathscr{Y}\mathscr{K}. \tag{34}$$

Proof. Let $\mathscr{Y}\mathscr{K} = \mathscr{M}\mathscr{K}$, and it is clear that

$$\begin{aligned}\mathscr{K} &= \mathscr{M}^{-1}\mathscr{Y}\mathscr{K}\\ &= \begin{bmatrix} \mathscr{M}_1^{-1} & 0 \\ 0 & \mathscr{M}_2^{-1}\end{bmatrix}\begin{bmatrix} I_p & 0 \\ 0 & 0\end{bmatrix}\mathscr{K},\end{aligned} \tag{35}$$

where $\mathscr{M}$ is a diagonal matrix. On account of the Schur complement, (32) is ensured in virtue of (16). □

4. Numerical Examples

This section exhibits a simulation example in order to evaluate the effectiveness of the given methodology, Figure 1 describes dynamic modes of the single-area power system. Note that the parameters are explained in Table 2 [35], and the matrix $\overline{B}$ is presupposed to be $\overline{B} = [0\ \ 0\ \ 1;\ 1\ \ 0\ \ 0;\ 0\ \ 1\ \ 0;\ 0\ \ 1\ \ 0]$.

We set the deception attack as $f(y(t)) = -\tanh(Fy(t))$, which $\mathscr{F} = \mathrm{diag}\{0.1, 0.1\}$. The actuator failure is supposed to be $\rho \in [0.8, 0.9]$ with $\underline{\rho} = 0.8$ and $\overline{\rho} = 0.9$. Other parameters are chosen as $\mathscr{S} = 3$, $\overline{\alpha} = 0.2$, $\overline{\sigma} = 0.1$, $\sigma = 0.015$, $\epsilon = 2$, $\iota = 0.1$, $d_M = 0.05$, and the sampling period $h = 0.02$.

In light of Theorem 2, the controller gain and the event-triggered matrix can be calculated:

$$\begin{aligned} K &= [\,1.8220 \ \ -1.0658\,],\\ \Omega &= \begin{bmatrix} 13.9953 & -0.9412 \\ -0.9412 & 8.7407 \end{bmatrix}. \end{aligned} \tag{36}$$

Specifically, we select the load disturbance as

$$\omega(t) = \begin{cases} 0.05\sin(t), \text{if } t \in [0,8], \\ 0, \text{if } t \in [8,\infty], \end{cases} \tag{37}$$

and the initial value is set as $\chi_0 = [-0.9 - 0.1 - 0.01 - 0.01]^{\top}$.

The numerical simulations of the system (16) are presented in Figures 2–6 using the aforementioned parameters

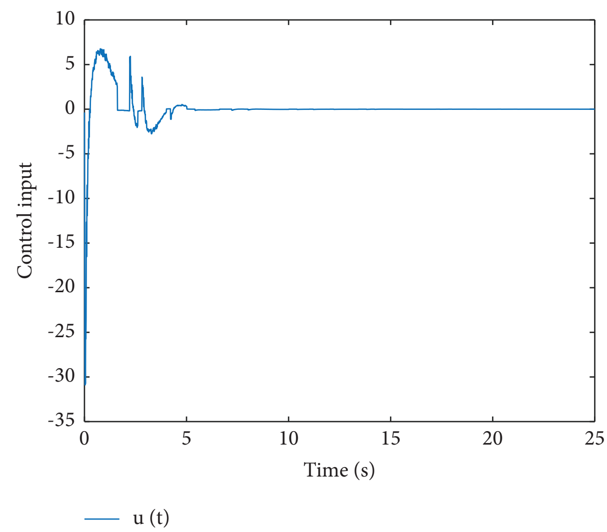

FIGURE 2: The control input $u(t)$.

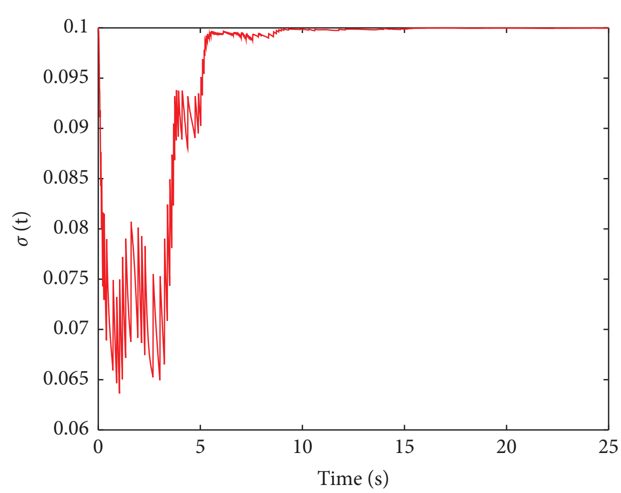

FIGURE 3: The evolution of the adaptive parameter $\sigma(t)$.

and assumptions. Figures 2 and 3 depict the control input $u(t)$ and the trend of the adaptive parameter (t). Figure 4 illustrates the deception attacks signals $\alpha(t)$ with the expectation $\overline{\alpha} = 0.2$. Additionally, to demonstrate the superiority of the proposed MAETP, we compared it with the METP of literature [18], as shown in Figures 5–7, where Figures 5 and 8 depict the power system state trajectory curves under different ETPs, respectively, and Figures 6 and

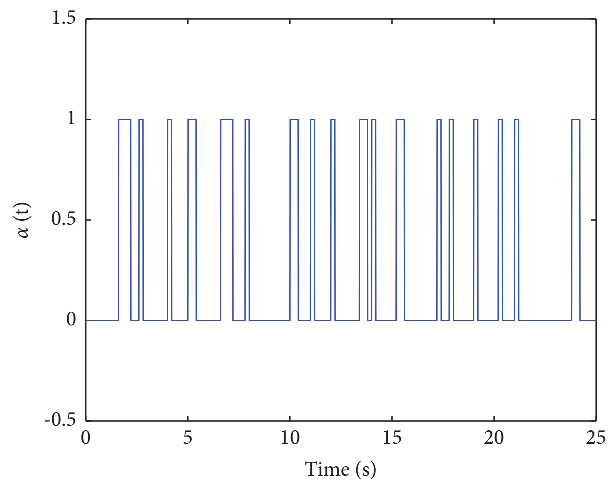

Figure 4: $\alpha(t)$ of deception attacks with $\overline{\alpha} = 0.2$.

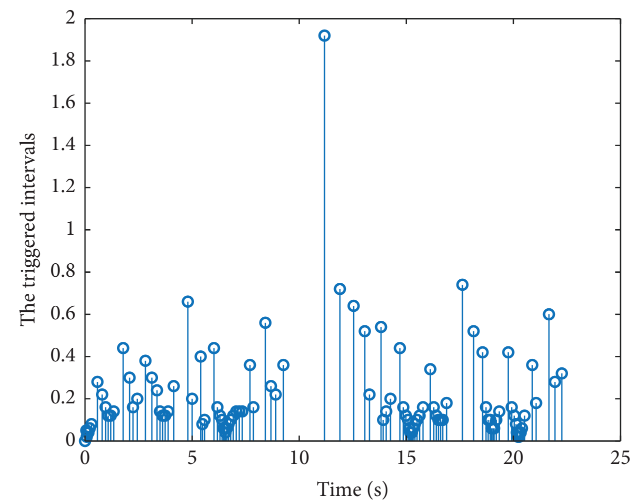

Figure 7: The triggering instants for METP.

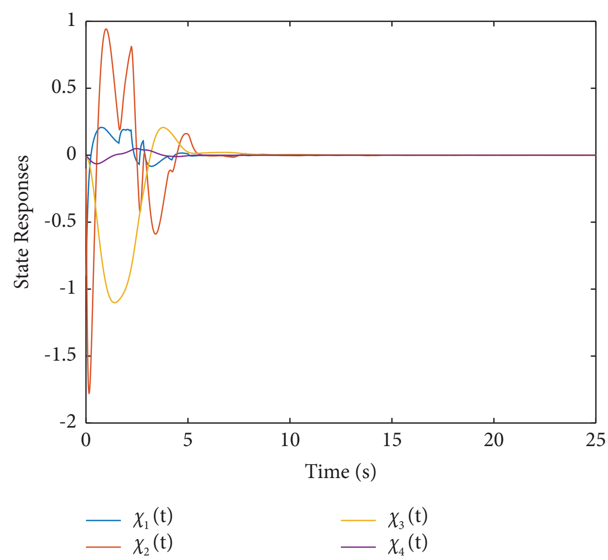

Figure 5: The state trajectories $\chi(t)$ for MAETP.

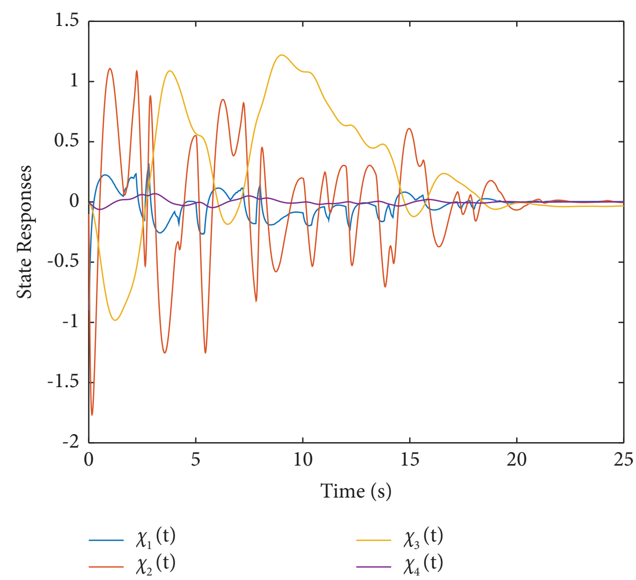

Figure 8: The state trajectories $\chi(t)$ for METP.

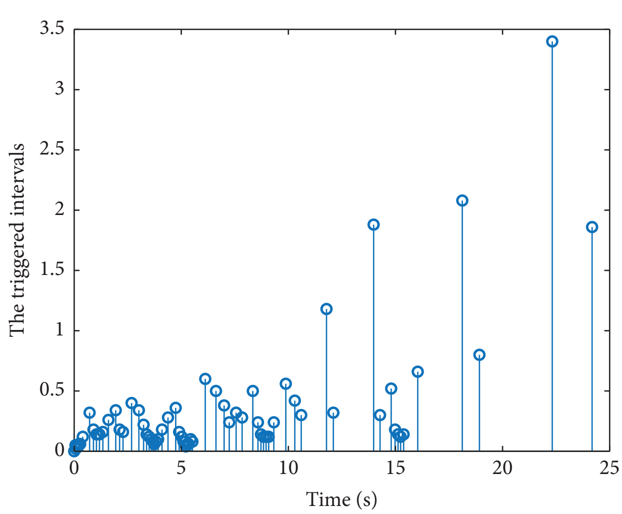

Figure 6: The triggering instants for MAETP.

7 correspond to their triggering instants. In Figures 5 and 8, it can be seen that the system curve takes less time to reach stability with the proposed MAETP. Furthermore, 108 packets have been transmitted under METS, while 68 packets have been transmitted under MAETS. Therefore, by comparison, it can be found that the proposed MAETP not only achieves good control performance but also saves transmission resources to a certain extent.

5. Conclusions

In this paper, a protocol-based LFC issue for SAPSs has been discussed. In light of the network's actual state, the networked power system is expanded to include actuator failures and deception attacks. Furthermore, by adaptively modifying the trigger thresholds based on historical sample data, MAETPs are developed to conserve network resources. By using Lyapunov function theory, sufficient criteria have been forwarded to guarantee the AS of SAPSs. In the end, an example has been applied to demonstrate the viability of the presented control scheme.

Data Availability

The data used to support the findings of this study are available from the corresponding author upon request.

Conflicts of Interest

The authors declare that they have no conflicts of interest.

References

[1] K. Lim, Y. Wang, and R. Zhou, “Robust decentralised load–frequency control of multi-area power systems,” *IEE Proceedings - Generation, Transmission and Distribution*, vol. 143, no. 5, pp. 377–386, 1996.

[2] H. A. Yousef, K. Al-Kharusi, M. H. Albadi, and N. Hosseinzadeh, “Load frequency control of a multi-area power system: an adaptive fuzzy logic approach,” *IEEE Transactions on Power Systems*, vol. 29, no. 4, pp. 1822–1830, 2014.

[3] L. Xie, J. Cheng, Y. Zou, Z.-G. Wu, and H. Yan, “A dynamic-memory event-triggered protocol to multiarea power systems with semi-markov jumping parameter,” *IEEE Transactions on Cybernetics*, pp. 1–11, 2022.

[4] C. Peng, J. Zhang, and H. Yan, “Adaptive event-triggering $$\{H\}$ \_ $\{$$\backslash$infty$\}$ $ load frequency control for network-based power systems,” *IEEE Transactions on Industrial Electronics*, vol. 65, no. 2, pp. 1685–1694, 2018.

[5] C.-K. Zhang, L. Jiang, Q. H. Wu, Y. He, and M. Wu, “Delay-dependent robust load frequency control for time delay power systems,” *IEEE Transactions on Power Systems*, vol. 28, no. 3, pp. 2192–2201, 2013.

[6] S. Wen, X. Yu, Z. Zeng, and J. Wang, “Event-triggering load frequency control for multiarea power systems with communication delays,” *IEEE Transactions on Industrial Electronics*, vol. 63, no. 2, pp. 1308–1317, 2016.

[7] Y. Zhang and T. Yang, “Decentralized switching control strategy for load frequency control in multi-area power systems with time delay and packet losses,” *IEEE Access*, vol. 8, Article ID 15838, 15850 pages, 2020.

[8] Q. Zhao and J. Jiang, “Reliable state feedback control system design against actuator failures,” *Automatica*, vol. 34, no. 10, pp. 1267–1272, 1998.

[9] W. Zhou, Y. Wang, C. K. Ahn, J. Cheng, and C. Chen, “Adaptive fuzzy backstepping-based formation control of unmanned surface vehicles with unknown model nonlinearity and actuator saturation,” *IEEE Transactions on Vehicular Technology*, vol. 69, no. 12, Article ID 14749, 14764 pages, 2020.

[10] H. Wang, P. X. Liu, X. Zhao, and X. Liu, “Adaptive fuzzy finite-time control of nonlinear systems with actuator faults,” *IEEE Transactions on Cybernetics*, vol. 50, no. 5, pp. 1786–1797, 2020.

[11] C. Deng and C. Wen, “Distributed resilient observer-based fault-tolerant control for heterogeneous multiagent systems under actuator faults and dos attacks,” *IEEE Transactions on Control of Network Systems*, vol. 50, no. 5, pp. 1786–1797, 2019.

[12] A. Humayed, J. Lin, F. Li, and B. Luo, “Cyber-physical systems security-a survey,” *IEEE Internet of Things Journal*, vol. 4, no. 6, pp. 1802–1831, 2017.

[13] Z. Guo, D. Shi, K. H. Johansson, and L. Shi, “Optimal linear cyber-attack on remote state estimation,” *IEEE Transactions on Control of Network Systems*, vol. 4, no. 1, pp. 4–13, 2017.

[14] F. Yang, Z. Gu, and S. Yan, “Switched event-based control for nonlinear cyber-physical systems under deception attacks,” *Nonlinear Dynamics*, vol. 106, no. 3, pp. 2245–2257, 2021.

[15] J. Liu, Y. Gu, L. Zha, Y. Liu, and J. Cao, “Event-Triggered $H_ \infty$ Load Frequency Control for Multiarea Power Systems under Hybrid Cyber Attackshooload frequency control for multiarea power systems under hybrid cyber attacks,” *IEEE Transactions on Systems, Man, and Cybernetics: Systems*, vol. 49, no. 8, pp. 1665–1678, 2019.

[16] Y. Zhu and W. X. Zheng, “Observer-based control for cyber-physical systems with periodic dos attacks via a cyclic switching strategy,” *IEEE Transactions on Automatic Control*, vol. 65, no. 8, pp. 3714–3721, 2020.

[17] Q. Sun, K. Zhang, and Y. Shi, “Resilient model predictive control of cyber-physical systems under dos attacks,” *IEEE Transactions on Industrial Informatics*, vol. 16, no. 7, pp. 4920–4927, 2020.

[18] E. Tian and C. Peng, “Memory-based event-triggering H ∞ load frequency control for power systems under deception attacksH∞load frequency control for power systems under deception attacks,” *IEEE Transactions on Cybernetics*, vol. 50, no. 11, pp. 4610–4618, 2020.

[19] L. Guo, H. Yu, and F. Hao, “Event-triggered control for stochastic networked control systems against denial-of-service attacks,” *Information Sciences*, vol. 527, pp. 51–69, 2020.

[20] H. Sun, C. Peng, T. Yang, H. Zhang, and W. He, “Resilient control of networked control systems with stochastic denial of service attacks,” *Neurocomputing*, vol. 270, pp. 170–177, 2017.

[21] F. Qu, E. Tian, and X. Zhao, “Chance-constrained state estimation for recursive neural networks under deception attacks and energy constraints: the finite-horizon casehstate estimation for recursive neural networks under deception attacks and energy constraints: the finite-horizon case,” *IEEE Transactions on Neural Networks and Learning Systems*, pp. 1–12, 2022.

[22] Y. Cui, Y. Liu, W. Zhang, and F. E. Alsaadi, “Sampled-based consensus for nonlinear multiagent systems with deception attacks: the decoupled method,” *IEEE Transactions on Systems, Man, and Cybernetics: Systems*, vol. 51, no. 1, pp. 561–573, 2021.

[23] J. Cheng, J. H. Park, X. Zhao, J. Cao, and W. Qi, “Static output feedback control of switched systems with quantization: a nonhomogeneous sojourn probability approach,” *International Journal of Robust and Nonlinear Control*, vol. 29, no. 17, pp. 5992–6005, 2019.

[24] J. Cheng, W. Huang, H.-K. Lam, J. Cao, and Y. Zhang, “Fuzzy-model-based control for singularly perturbed systems with nonhomogeneous Markov switching: a dropout compensation strategy,” *IEEE Transactions on Fuzzy Systems*, vol. 30, no. 2, pp. 530–541, 2022.

[25] J. Cheng, Y. Shan, J. Cao, and J. H. Park, “Nonstationary control for t–s fuzzy Markovian switching systems with variable quantization density,” *IEEE Transactions on Fuzzy Systems*, vol. 29, no. 6, pp. 1375–1385, 2021.

[26] C. Peng and T. C. Yang, “Event-triggered communication and h∞control co-design for networked control systems,” *Automatica*, vol. 49, no. 5, pp. 1326–1332, 2013.

[27] J. Cheng, L. Liang, J. H. Park, H. Yan, and K. Li, “A dynamic event-triggered approach to state estimation for switched memristive neural networks with nonhomogeneous sojourn

probabilities," *IEEE Transactions on Circuits and Systems I: Regular Papers*, vol. 68, no. 12, pp. 4924–4934, 2021.

[28] P. Shi, H. Wang, and C.-C. Lim, "Network-based event-triggered control for singular systems with quantizations," *IEEE Transactions on Industrial Electronics*, vol. 63, no. 2, pp. 1230–1238, 2016.

[29] J. Cheng, Y. Wu, Z. Wu, and K. Li, "Fuzzy filter design for affine systems with sensor faults: a dynamic event-triggered approach," *Journal of Systems Science and Complexity*, vol. 35, no. 5, pp. 1761–1784, 2022.

[30] S. Zhu, E. Tian, D. Xu, and J. Liu, "An adaptive torus-event-based controller design for networked t-s fuzzy systems under deception attacks," *International Journal of Robust and Nonlinear Control*, vol. 32, no. 6, pp. 3425–3441, 2022.

[31] L. Zha, R. Liao, J. Liu, X. Xie, E. Tian, and J. Cao, "Dynamic event-triggered output feedback control for networked systems subject to multiple cyber attacks," *IEEE Transactions on Cybernetics*, vol. 52, no. 12, pp. 13800–13808, 2022.

[32] Z. Gu, P. Shi, and D. Yue, "An adaptive event-triggering scheme for networked interconnected control system with stochastic uncertainty," *International Journal of Robust and Nonlinear Control*, vol. 27, no. 2, pp. 236–251, 2017.

[33] X. Xie, S. Li, and B. Xu, "Adaptive event-triggered H∞ fuzzy filtering for interval type-2 T–S fuzzy-model-based networked control systems with asynchronously and imperfectly matched membership functions," *Journal of the Franklin Institute*, vol. 356, no. 18, pp. 11760–11791, 2019.

[34] X.-G. Guo, X. Fan, J.-L. Wang, and J. H. Park, "Event-triggered switching-type fault detection and isolation for fuzzy control systems under dos attacks," *IEEE Transactions on Fuzzy Systems*, vol. 29, no. 11, pp. 3401–3414, 2021.

[35] H. Zhang, J. Liu, and S. Xu, "H-infinity load frequency control of networked power systems via an event-triggered scheme," *IEEE Transactions on Industrial Electronics*, vol. 67, no. 8, pp. 7104–7113, 2020.

[36] Y. Tian, H. Yan, H. Zhang, J. Cheng, and H. Shen, "Asynchronous output feedback control of hidden semi-markov jump systems with random mode-dependent delays," *IEEE Transactions on Automatic Control*, vol. 67, no. 8, pp. 4107–4114, 2022.

[37] P. Park, J. W. Ko, and C. Jeong, "Reciprocally convex approach to stability of systems with time-varying delays," *Automatica*, vol. 47, no. 1, pp. 235–238, 2011.